

# Neutronics Assessment of a Compact D-D Neutron Generator as a Neutron Source for the Neutron Calibration in Magnetic Confinement Fusion Devices<sup>\*)</sup>

Takeo NISHITANI, Roman RODIONOV<sup>1)</sup>, Vitaly KRASILNIKOV<sup>2)</sup>, Aakanksha SAXENA<sup>2)</sup>,  
Laura CORE<sup>2)</sup> and Luciano BERTALOT<sup>2)</sup>

*National Institute for Fusion Science, National Institutes of Natural Sciences, 322-6 Oroshi-cho, Toki 509-5292, Japan*

<sup>1)</sup>*Project Center ITER, Moscow, 123182, Russia*

<sup>2)</sup>*ITER Organization, 3067 St Paul Lez Durance Cedex, France*

(Received 26 November 2019 / Accepted 1 March 2020)

Neutronics aspects of a compact D-D neutron generator as a neutron source for the neutron calibration in magnetic confinement fusion devices are assessed by the MCNP calculation. The neutron emission distribution of the compact D-D neutron generator has a large anisotropy not only due to the scattering with the neutron generator body but also due to the intrinsic anisotropy of the differential cross-section of the  $d(d,n)^3\text{He}$  reaction. The angular neutron distribution at the target of the compact D-D neutron generator is calculated with the PHITS code where the slowing down on the accelerated deuterons in the target material is considered. The calibration experiments are simulated by using the MCNP-6 code for the ITER neutron flux monitor (NFM) to be installed in the equatorial port. The detection efficiency of NFM is calculated for a D-D plasma neutron source, an idealistic D-D neutron source, a  $^{252}\text{Cf}$  neutron source and the compact neutron generator. It is found that the detection efficiency of NFM for the compact neutron generator is approximately 50% larger than that for the idealistic D-D neutron source. The discrepancy is improved to be 25% by the intention of the target 20 cm from the body of the compact neutron generator.

© 2020 The Japan Society of Plasma Science and Nuclear Fusion Research

Keywords: neutron calibration, compact neutron generator, neutronics, MCNP-6, PHITS, neutron flux monitor

DOI: 10.1585/pfr.15.2402017

## 1. Introduction

A neutron flux monitor (NFM) is one of the most important diagnostics in the D-D or D-T plasma experiment in order to evaluate the total fusion power. The calibration of neutron flux monitors against the total neutron emission rate in the whole plasma is one of the most important issues of the neutron measurement on magnetic confinement fusion devices. For the device with deuterium plasma operation, a  $^{252}\text{Cf}$  neutron source is commonly used in the in-situ calibration experiment, where the neutron moves in the toroidal direction inside the vacuum vessel, because the  $^{252}\text{Cf}$  neutron source [1–4] has an isotropic neutron emission with the average energy of 2.1 MeV. On the other hand, a compact D-T neutron generator has been used for D-T plasma operating devices such as TFTR [5] and JET [6], and will also be used in ITER. A compact D-D neutron generator has a possibility to be used at the neutron calibration for the deuterium operation phase prior to the D-T operation phase. The neutron calibration with the compact D-D neutron generator is a good practice of the D-T neutron calibration where the compact D-T neutron gener-

ator is used. However, the compact D-D neutron generator has a large anisotropy of the neutron emission due to the anisotropy of the  $D(d,n)^3\text{He}$  differential cross-section and the scattering/absorption by the neutron generator structure itself. Table 1 summarizes the advantage and the disadvantage of the  $^{252}\text{Cf}$  neutron source and the compact D-D neutron generator as the neutron source of the D-D neutron calibration experiment. Here, neutronics assessment of the compact D-D neutron generator has been performed compared with the conventional  $^{252}\text{Cf}$  neutron source by using the MCNP-6 [7] code with the FENDL-3.1 [8] nuclear library.

## 2. Neutronic Characterization of the Compact D-D Neutron Generator

ITER has a plan to use a compact neutron generator type NG24 m developed in Russian Federation as the neutron source in the D-D neutron calibration experiment. Figure 1 shows the schematics view of the NG24 m neutron generator [9]. An ion source and the target are mounted in the neutron generator body. The target is a thin Titanium layer on the copper substrate. The typical thickness of the Titanium layer is 10  $\mu\text{m}$ .

author's e-mail: nishitani.takeo@nifs.ac.jp

<sup>\*)</sup> This article is based on the presentation at the 28th International Toki Conference on Plasma and Fusion Research (ITC28).

Table 1 Comparison of  $^{252}\text{Cf}$  neutron source and DD compact neutron generator.

Property	$^{252}\text{Cf}$ neutron source	D-D compact neutron generator
Absolute intensity	Well known	Should be calibrated
Intensity stability	Stable	Should be monitored
Energy spectrum	Well known	Should be measured
Weight	Light	Heavy
Radiation safety during transportation	Shielding required	Safe
As a dry run for D-T calibration using D-T neutron generator	Poor	Good

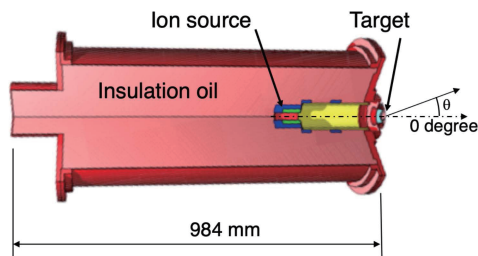


Fig. 1 Schematic view of the compact D-D neutron generator.

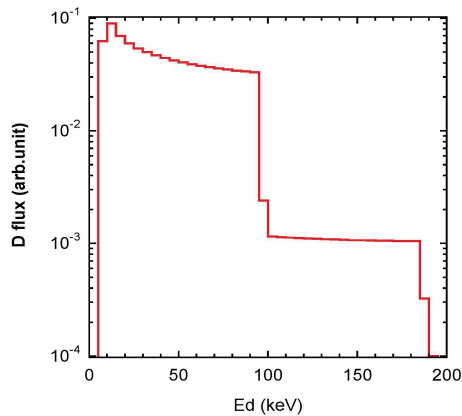


Fig. 2 Deuteron energy spectrum in the Target, where acceleration voltage is 180 keV, and beam species are  $\text{d}^+$  (10%) and  $\text{d}_2^+$  (90%).

Accelerated deuteron will make  $\text{D}(\text{d}, \text{n})^3\text{He}$  reaction with the deuterium in the Ti target, which is self-loaded by the deuteron beam. The typical acceleration voltage is 180 kV, and the beam species are  $\text{d}^+$  (10%) and  $\text{d}_2^+$  (90%). The accelerated deuterons are decelerated in the target material, therefore, the generated neutron energy is not monoenergetic. The deuteron energy spectrum is calculated by the PHITS code [10] as shown in Fig. 2.

Also, the angular dependent neutron spectra at the target is evaluated by the PHITS code. The PHITS code calculates the reaction rate and the emitted particle energy according to the nuclear reaction model. However, the ac-

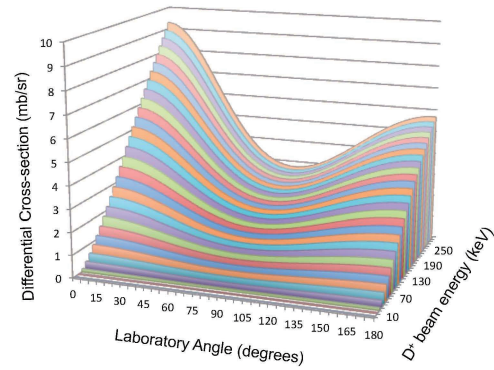


Fig. 3 Differential cross-section of the  $\text{D}(\text{d}, \text{n})^3\text{He}$  reaction as a function of the incident deuteron energy. Here, 0 degree is the incident direction of the  $\text{D}^+$  beam.

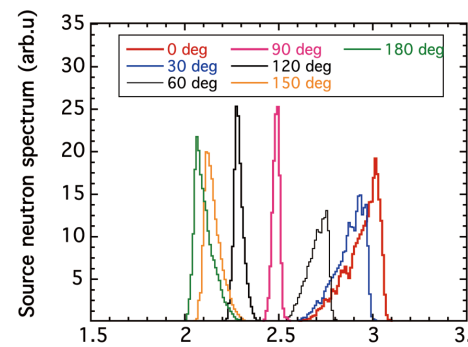


Fig. 4 Angular dependent neutron spectra at the target of the compact D-D neutron generator calculated by the PHITS code with double differential cross-section table for the  $\text{D}(\text{d}, \text{n})^3\text{He}$  reaction. The emission angle is  $\theta$  in Fig. 1.

curacy of the reaction model is poor for the light target nucleus and low incident energy lower than several MeV reactions. Here, the double differential cross-section table of the  $\text{D}(\text{d}, \text{n})^3\text{He}$  reaction is created by the kinematics and the differential cross-section recommended by IAEA [11]. The differential cross-section of the  $\text{D}(\text{d}, \text{n})^3\text{He}$  reaction is shown in Fig. 3, which indicates that the anisotropy increases with the incident deuteron energy. The PHITS code reads the double differential cross-section table for the  $\text{D}(\text{d}, \text{n})^3\text{He}$  reaction. Figure 4 shows the calculated angular dependent neutron spectra at the target of the compact D-D neutron generator. The neutron spectrum is quasi monoenergetic at 90 degrees. For the other angles, the neutron spectra have low or high energy tails due to the slowing down of deuterons in the target. In the forward direction, the maximum energy is approximately 3 MeV. On the other hand, the minimum energy is approximately 2 MeV in the backward direction.

Prior to the in-site calibration experiment, characterization measurement of the compact D-D neutron generator is planned, where the angular neutron spectra and the absolute neutron fluxes are determined. Here, angular neutron spectra are evaluated by the MCNP-6 code with the

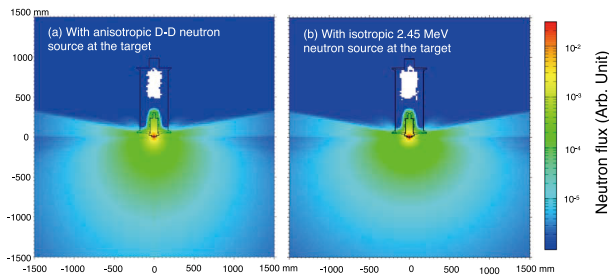


Fig. 5 Contour maps of the neutron flux around the neutron generator with the anisotropic D-D neutron source shown in Fig. 4 and the isotropic 2.45 MeV neutron source at the target.

geometrical model of the compact D-D neutron generator shown in Fig. 1. In the calculation, neutrons are generated at the center of the target surface with the angular spectra as shown in Fig. 4. The angular neutron spectra are evaluated at the location 2.5 m from the neutron source point from 0 to 180 degrees against the axis of the neutron generator with one degree pitch. Also, the neutron flux around the neutron generator is calculated. Figure 5 shows the contour map of the neutron flux around the neutron generator with the anisotropic D-D neutron source shown in Fig. 4 and the isotropic 2.45 MeV neutron source at the target. It is clearly recognized that the neutron flux is enhanced in the forward direction in the case of the anisotropic D-D neutron source at the target. Also, the neutron flux is decreased in the backward direction due to the absorption and the scattering by the insulation oil of the neutron generator in both cases.

### 3. Simulation of In-Situ Calibration Experiment

In-situ D-D neutron calibration experiment of ITER is simulated by the MCNP-6 code for different neutron source. In ITER, several kinds of NFMs are employed [12]. NFM in the equatorial port (EQ) #1 is regarded as the primary NFM for the fusion power measurement, because the detection location is the closest to the plasma. NFM in EQ#1 consists of the three fission chambers including 2 g, 0.2 g, and 0.02 g of  $^{235}\text{U}$ , respectively, and one dummy chamber as shown in Fig. 6. In many other fusion devices, the  $^{235}\text{U}$  fission chamber uses a Polyethylene moderator to increase the sensitivity for fast neutrons. However, Polyethylene is not applicable for the moderator of the ITER NFM in EQ#1, because the environmental temperature is higher than 200°C. Therefore,  $^{235}\text{U}$  fission chambers are surrounded with a Beryllium moderator. Here, we consider that 2 g  $^{235}\text{U}$  fission chamber is used as the neutron detector in the neutron calibration experiment, because it has the highest sensitivity.

For the MCNP simulation of the neutron calibration experiment, a simplified 20 degrees sector model is newly prepared as shown in Fig. 7, where the vacuum vessel,

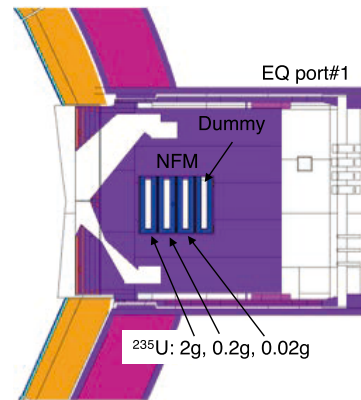


Fig. 6 Schematic view of ITER neutron flux monitor (NFM) in the equatorial port (EQ) #1 (vertical cut view).

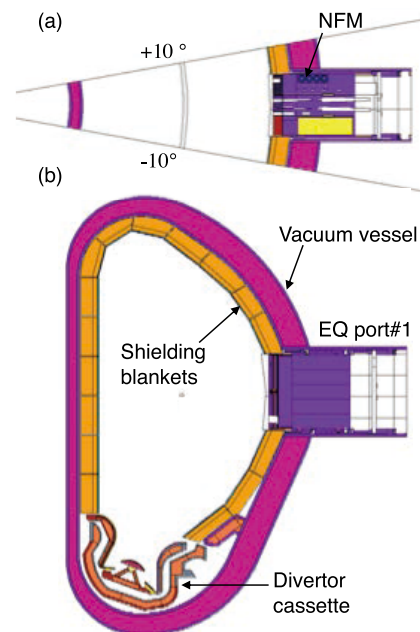


Fig. 7 Simplified ITER model for the MCNP calculation, (a) horizontal cut view and (b) vertical cut view.

shielding blankets and divertor cassettes are modeled. Because neutrons generated inside the vacuum vessel will reach the NFM directory or by scattering with in-vessel components, components outside the vacuum vessel are not important. The vacuum vessel and the in-vessel components are toroidally symmetric in order to save the computational time. On the other hand, a very precise model of the EQ#1 structure is employed from the ITER organization, because the surrounding structure of NFM is very important to evaluate the detection efficiency of NFM. The boundary surfaces at  $\pm 10$  degrees are reflection surfaces.

The detection efficiency of the NFM (2 g  $^{235}\text{U}$  fission chamber) is calculated for a D-D plasma neutron source, an idealistic D-D neutron source, a  $^{252}\text{Cf}$  neutron source, and the compact D-D neutron generator. The neutron source profile of the plasma neutron source is assumed to be the

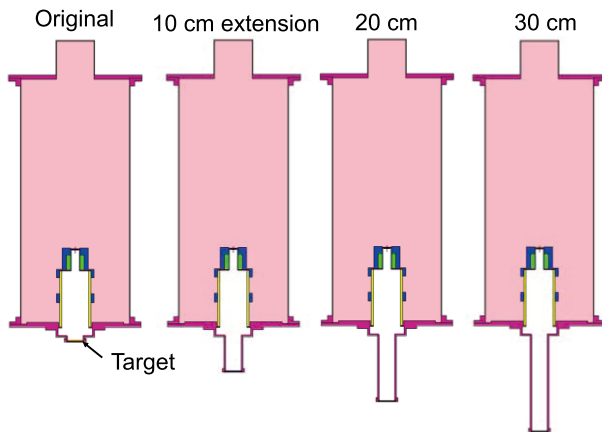


Fig. 8 Calculation models of the original and target extended compact D-D neutron generators.

Table 2 Detection efficiencies for different neutron sources.

Neutron source	Detection efficiency (Counts/source neutron)
D-D plasma	$5.11 \times 10^{-9}$
Idealistic D-D ring	$5.73 \times 10^{-9}$
$^{252}\text{Cf}$ ring	$4.90 \times 10^{-9}$
NG (original) ring	$8.75 \times 10^{-9}$
NG (+10 cm) ring	$7.52 \times 10^{-9}$
NG (+20 cm) ring	$7.18 \times 10^{-9}$
NG (+30 cm) ring	$7.01 \times 10^{-9}$

\*NG: Compact D-D neutron generator

same as the neutron source profile of the standard D-T ITER plasma. The ion temperature is 10 keV. Also, the idealistic D-D neutron source has a neutron spectrum of the 10 keV D-D plasma. In Section 2, we found that the absorption and the scattering by the insulation oil was remarkable. Thus, not only the original compact D-D neutron generator but also extended target options are considered as shown in Fig. 8. In the cases of the idealistic D-D neutron source, the  $^{252}\text{Cf}$  neutron source, and the compact D-D neutron generator, point neutron sources are located at toroidal positions with a one-degree pitch on the magnetic axis of the 6.2 m major radius in order to simulate the ring neutron source. The target position of the compact D-D neutron generator is on the magnetic axis of the torus, where the axis of the compact D-D neutron generator is the outward radial direction.

Table 2 shows the detection efficiency for the D-D plasma neutron source, and quasi ring sources of the idealistic D-D neutron source, the  $^{252}\text{Cf}$  neutron source, and four kinds of the compact D-D neutron generators. In JT-60U and LHD, calculated detection efficiency for the D-D plasma neutron source, the idealistic D-D neutron ring source, and the  $^{252}\text{Cf}$  neutron ring source are very close, typically  $\pm 5\%$ . However, discrepancies among those detection efficiencies are 10% or larger in ITER. This is probably because NFM is too close to the plasma, thus the detection efficiency is affected by the neutron source profile

and the neutron energy.

Also, the detection efficiency for the original compact D-D neutron generator is approximately 50% larger than that for the idealistic D-D neutron source. If we extend the target additionally 10, 20, and 30 cm, the discrepancy will be reduced to approximately 30, 25, and 22%, respectively. Therefore, we would like to propose to use the target extended compact D-D neutron source in the case that the compact D-D neutron generator is employed in the D-D neutron calibration experiment. From the accuracy point of view, the  $^{252}\text{Cf}$  neutron source is preferable. However, we have to consider many aspects in the choice of the neutron source as discussed in Section 1. If the compact neutron generator is employed, the precise characterization of the neutron source such as angular neutron intensities and the spectra must be evaluated experimentally. Also, the precise evaluation of the relationship between the detection efficiency derived from the compact neutron generator and that for the plasma neutron source by the calculation with more precise model.

## 4. Summary

The advantage and the disadvantage of the  $^{252}\text{Cf}$  neutron source and the compact D-D neutron generator is discussed for the neutron source of the D-D neutron calibration experiment. Angular neutron spectra from the compact D-D neutron generator are evaluated by using the MCNP-6 code based on the target neutron spectra calculated by the PHITS code considering the slowing down of deuterons in the target material. The detection efficiency of NFM is calculated for the D-D plasma neutron source, the idealistic D-D neutron source, the  $^{252}\text{Cf}$  neutron source and the compact neutron generator. From the accuracy point of view, the  $^{252}\text{Cf}$  neutron source is preferable. In the case of the compact D-D neutron generator, large discrepancy between detection efficiencies for the D-D plasma source and the compact D-D neutron generator must be carefully considered.

## Acknowledgments

This work was supported by the ITER Scientist Fellow arrangement (ITER\_D\_WDW5WH).

- [1] H.W. Hendel *et al.*, Rev. Sci. Instrum. **61**, 1900 (1990).
- [2] O.N. Jarvis *et al.*, Rev. Sci. Instrum. **61**, 3172 (1990).
- [3] T. Nishitani *et al.*, Rev. Sci. Instrum. **63**, 5270 (1992).
- [4] T. Nishitani *et al.*, Fusion Eng. Des. **136**, 210 (2018).
- [5] L.C. Johnson *et al.*, Rev. Sci. Instrum. **66**, 894 (1995).
- [6] P. Batistoni *et al.*, Nucl. Fusion **58**, 106016 (2018).
- [7] D.B. Pelowitz (Ed.), LA-CP-13-00634, Los Alamos National Laboratory (2013).
- [8] A. Koning *et al.*, <https://www-nds.iaea.org/fendl/>
- [9] Y. Kashchuk, private communication.
- [10] T. Sato *et al.*, J. Nucl. Sci. Technol. **50**, 913 (2013).
- [11] M. Drosig *et al.*, INDC(AUS)-0019, IAEA (2015).
- [12] L. Bertalot *et al.*, J. Instrum. **7**, C04012 (2012).